

**SOFT TISSUE
SOLITARY FIBROUS
TUMOR.
IMAGING FINDINGS IN
A SERIES OF NINE
CASES.**

AUTOR: JOSEP GARCIA BENNETT

DIRECTOR DEL TREBALL: DR JOSE CÁCERES SIRGO

TREBALL DE RECERCA UNIVERSITAT AUTÒNOMA
BARCELONA

AUGUST 2010, BARCELONA

Index

| | |
|--|----|
| Introduction | 3 |
| Histological background of solitary fibrous tumors | 4 |
| Subjects and Methods | 9 |
| Results | |
| Clinical Results | 10 |
| Surgical and Pathological Results | 11 |
| Imaging Findings | 12 |
| Figures | 14 |
| Discussion | 22 |
| References | 24 |

Introduction

Soft tissue solitary fibrous tumors (SFT) are rare mesenchymal neoplasms of ubiquitous location. This tumor was thought to only affect serous tissues, specially the pleura. In the last 20 years SFTs have been reported in almost every anatomic location. In a recent classification on soft tissue neoplasms, different tumors have been added to this entity (1).

The relation between pathological morphology and clinical outcome is poor (2). All this makes the management of this tumor a challenging task for both clinicians and pathologists. Radiological information may provide some useful information.

Few articles have been published regarding the radiological characteristics of this tumor. To our knowledge only one large series study has been reported (4). The rest of the literature is focused on case reports (5-13).

The aim of this study is to describe the radiological features of this tumor in a series of nine patients and to compare these results with pathological correlation and clinical outcome.

Histological background of solitary fibrous tumors

In the last twenty years the classification of solitary fibrous tumors (SFT) and haemangiopericytomas (HPC) has changed.

The term haemangiopericytoma was first described by Stout and Murray in 1942 as “tumors composed of capillary blood vessels with one or more layers of rounded cells arranged about them, which have a certain cytological similarities with pericytes”. Since then, the term haemangiopericytoma has been used very loosely. Today, pathologists prefer to use it as a descriptive characteristic rather than a true entity. There are a number of reasons for doing this. First, many benign and malignant tumors show morphological features of HPC, not being specific for a unique entity. Second, it appears that the cells of most tumors labeled as HPC in fact show no pericytic differentiation ultrastructurally and don't express typical pericytic proteins (muscle-specific actin, (HHF-35) or smooth muscle actin). The third reason is the difficulty in predicting the clinical behavior of these tumors. Those that show obvious malignant features at pathological examination behave more aggressively. The problem arises in benign looking lesions, of which a small percentage can recur or metastasize.

Most of the tumors labeled as HPC have now been reclassified and are thought to be a cellular variant of solitary fibrous tumors. Even at the meninges where HPC tumors were regarded as a unique entity, new data suggests that they are indistinct to the cellular variant of SFT. Lipomatous haemangiopericytomas and giant cell angiofibromas are also thought to be variants of SFT (2).

Tumors arising from pericytes do exist and include glomangiopericytoma /myopericytoma, infantile myofibromatosis and a subset of sinonasal HPCs.

Conventional SFTs were thought to only arise in serous superficies, specially the pleura. In the past 20 years, this tumor has been described in almost every location in the body. These tumors have a distinct pathological pattern with HPC-like features and are now classified as fibrous variants of SFT.

In conclusion, the term solitary fibrous tumor today encloses two main subtypes, a cellular form (derived from HPCs) and a fibrous form (derived from conventional SFTs). Cellular forms have a monotonous microscopic appearance with moderate to high cellularity and with little intervening fibrosis. Thin-walled branching vessels are visible. The cells express CD34 but with less intensity compared to the fibrous forms.

The fibrous form has a heterogeneous microscopic appearance, alternating cellular and fibrous areas, separated by thick walled vessels (Figures 2). The cells are fusiform in shape (Figure 3) and are strongly immunoreactive for CD34 (Figure 4).

Macroscopically the tumors are well margined, partially encapsulated masses, measuring between 1 and 25 cm (Figure 1). On cut section they have a multinodular whitish firm appearance with occasional myxoid and hemorrhagic

changes. Necrosis and infiltrative margins are observed in locally aggressive or malignant tumors (1)

The behavior of SFT is unpredictable and roughly 10-15% show malignant behavior in the form of recurrence or metastasis. Metastasis occurs in the lungs, liver and bone. The relationship between pathological morphology and clinical behavior is poor.

Some studies suggest that the cellular form behaves more aggressively than the fibrous one, developing metastasis more frequently (2).



Figure 1. Cut section of surgical specimen showing a multinodular partially encapsulated mass

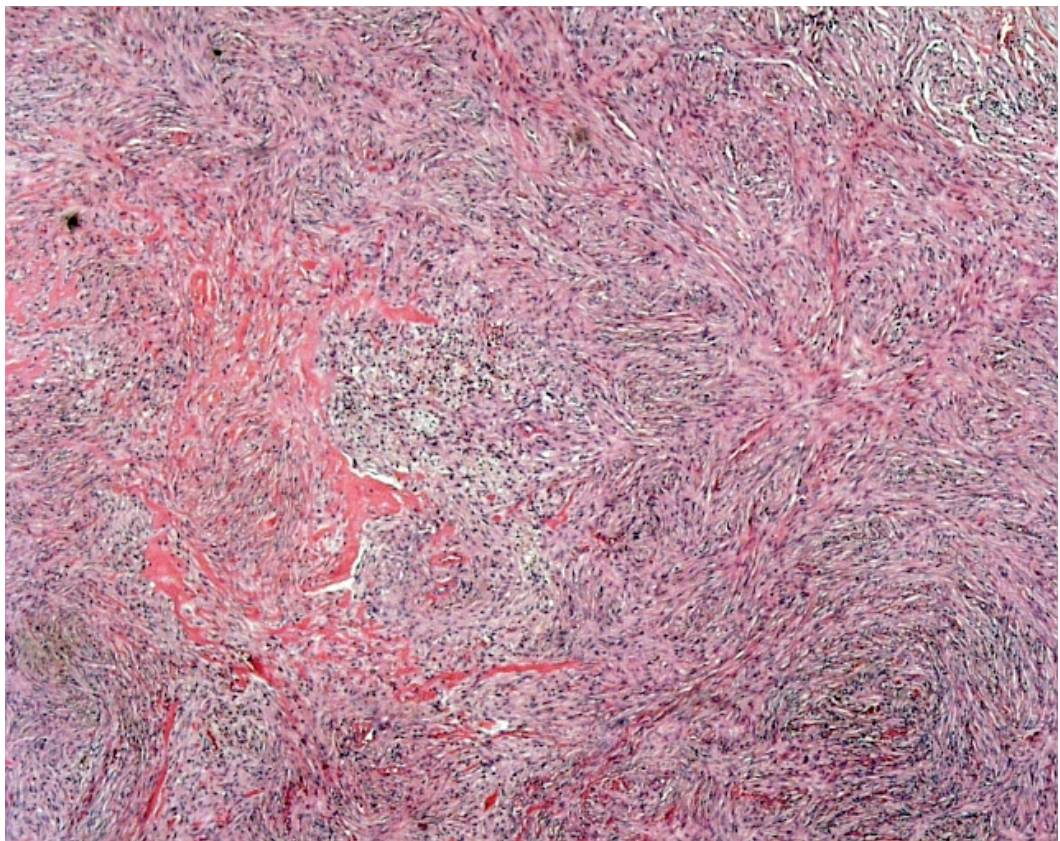


Figure 2. Storiform pattern with collagen bands (fibrous form)

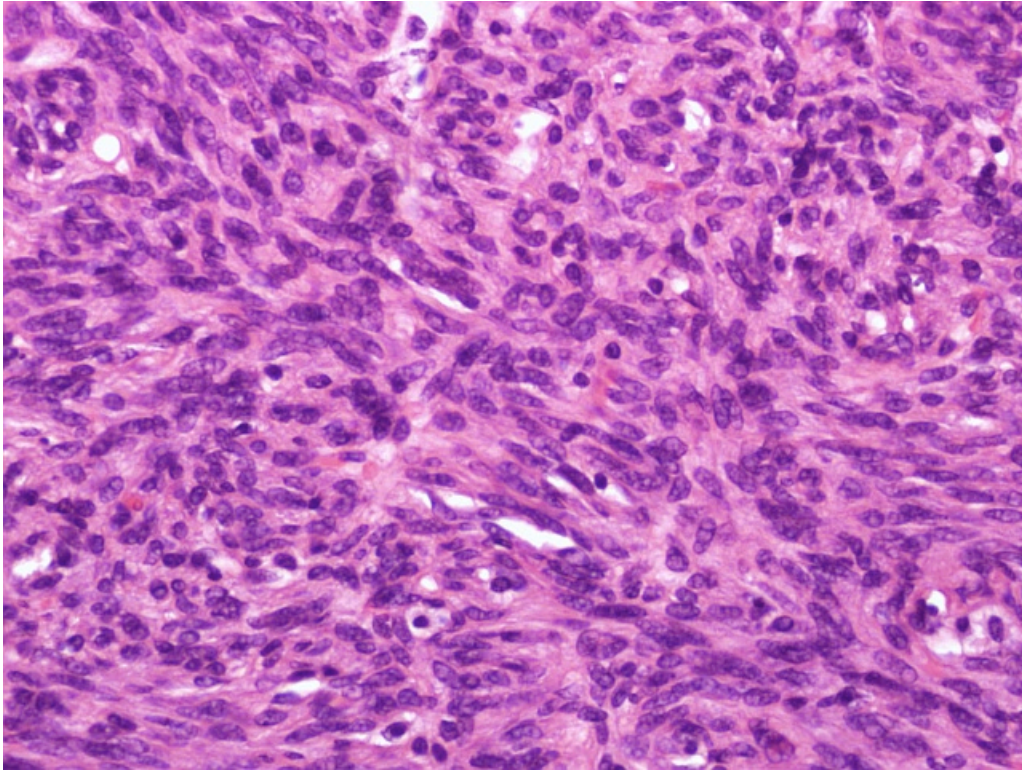


Figure 3. Fusiform cells showing no atipia or mitosis.

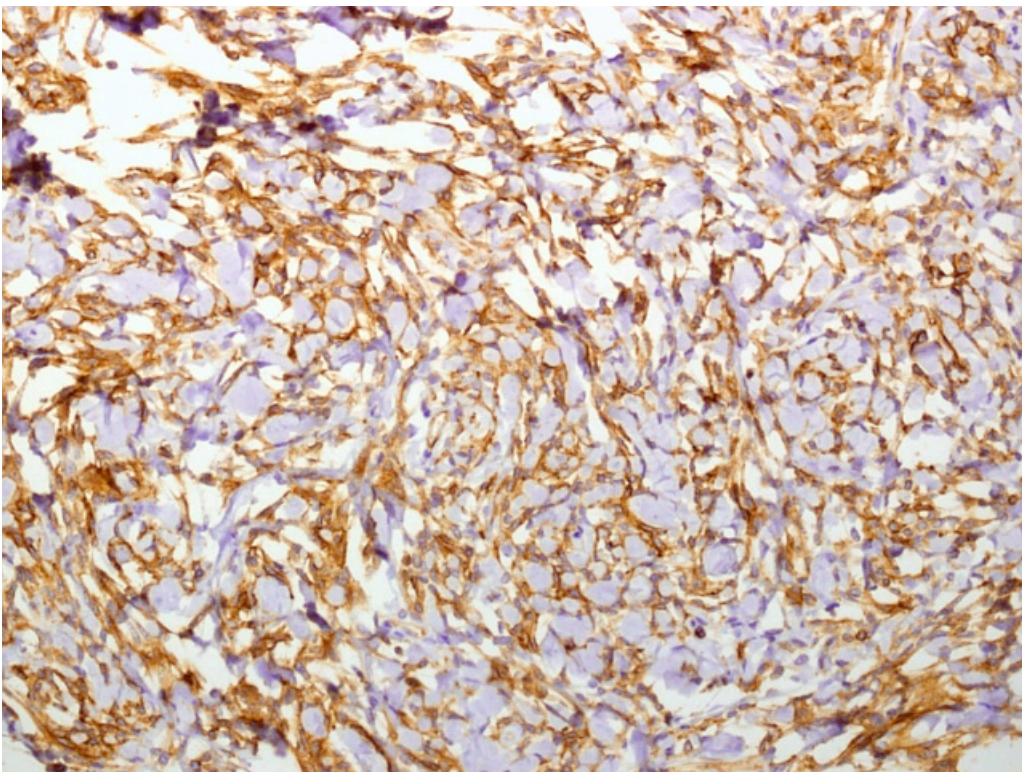


Figure 4. CD34 expression on tumor cells.

Subjects and Methods

A review of 17 cases confirmed pathologically by an experienced soft-tissue tumor pathologist was carried out in our institution between 1993 and 2008.

All imaging studies were collected for analysis. Tumors that affected visceral organs, thoracic pleura and the central nervous system were rejected from the study.

Nine cases (9/17) of soft tissue tumors were studied through imaging (CT, MRI and ultrasound) and form the basis of this study (table 1). Age ranged between 38 and 77, and there was a female predilection (7/9) (table 1)

Tumor location, size, morphology, local invasion, vascularity, contrast enhancement and MRI signal intensities were recorded. Tumor vascular angiogenesis was studied in four patients with dynamic contrast enhanced MRI. Clinical information, including patient age, sex, and clinical presentation were also recorded.

Table 1

| Case | Age | Sex | Location | RX | US | CT | MRI | DCE |
|-------------|------------|---------------|------------------------|-----------|-----------|-----------|------------|------------|
| 1 | 38 | Female | Thoracic wall | | X | X | X | X |
| 2 | 46 | Male | Arm | | X | | X | X |
| 3 | 73 | Male | Retroperitoneum | | X | X | | |
| 4 | 58 | Female | Thigh | X | X | X | X | X |
| 5 | 50 | Female | Thigh | | X | | | |
| 6 | 76 | Female | Pectoral | | X | X | X | |
| 7 | 77 | Female | Knee | | | | X | X |
| 8 | 68 | Female | Thoracic wall | X | X | | X | |
| 9 | 39 | Female | Thigh | | X | | | |

Pathological criteria for malignancy were evaluated in surgical specimens. Those tumors that showed infiltrative margins, high cellularity, nuclear pleomorphism, areas of tumor necrosis and an increased mitotic index (> 4 mitosis per 10 HPF) were regarded as malignant.

Results

Clinical results

The clinical findings of these patients are summarized on table 2.

The locations of these tumors were the following: 5 (55%) in the extremities, 3 (33%) in the soft tissues of the trunk and 1 (11%) in the retroperitoneum. The size of the lesions varied between 2,5 cm and 22 cm (mean 9.5). Four (44%) tumors were larger than 10 cm in size.

The clinical presentation of all cases was a growing mass. Pain was only recorded in 4 patients (44%). Those tumors that caused pain had a mean size of 13.4 cm whilst those that didn't of 5.3 cm.

Metastasis at the moment of diagnosis was observed in one only tumor, which presented malignant criteria at pathological analysis. The location of the metastasis was in the bone but later it developed in the lung

Patients were followed for 2-5 years. Recurrence occurred twice in the same patient at the surgical site (case 2, Figure 9). This tumor did not show malignant characteristics at pathology.

Table 2

| Case | Location | Size (cm) | Pain | Presurgery biopsy | Malignant criteria | Metastasis | Follow up (y) | Recurrence |
|--------------|-----------------|------------------|-------------|--------------------------|---------------------------|-------------------|----------------------|-------------------|
| 1 | Thoracic wall | 6 | No | Yes | No | No | 2 | No |
| 2 | Arm | 4,2 | Yes | No | No | No | 3 | Yes |
| 3 | Retroperitoneum | 10,8 | No | No | No | No | 2 | No |
| 4 | Thigh | 22 | Yes | Yes | Yes | Yes | 3 | No |
| 5 | Thigh | 2 | No | Yes | No | No | 5 | No |
| 6 | Pectoral | 10,5 | No | Yes | No | No | 3 | No |
| 7 | Knee | 6,5 | Yes | No | No | No | 2 | No |
| 8 | Thoracic wall | 21 | Yes | No | Yes | No | 2 | No |
| 9 | Thigh | 2,5 | No | No | No | No | 2.5 | No |
| Total | | 2-22 | 4 | 4 | 2 | 1 | 2-5 | 1 |

Surgical and Pathological Results

Core-biopsy guided by ultrasound was performed in 4 patients with a yield of 3 benign SFTs and one high grade fusocelular sarcoma.

All tumors were removed with wide margin surgery. In two of them adjuvant chemotherapy and radiotherapy was carried out. In one case, embolization prior surgery was performed to prevent excessive surgical hemorrhage.

Only two patients presented malignant criteria at pathological analysis of the surgical specimen (case 4 and 8).

Imaging findings

Nine patients in total were studied with imaging techniques (table 1).

Eight (8/9) patients were studied with ultrasound using a multifrequency (7,2-11,4 Mhz) transducer and Power Doppler signal optimized for low flow speeds and superficial lesions (Antares Acuson, Siemmens).

All lesions presented as a well-defined nodule or mass with either a homogeneous hypoechoic pattern (6 cases) or a predominantly hypoechoic pattern with heterogeneous areas (2 cases) (Figures 5 and 6). These last two were classified as malignant.

A vascular pedicle was recognized in all lesions. The power Doppler intratumoural signal showed either a peripheral pattern (4 cases) or a diffuse pattern (4 cases) (Figures 6 and 7).

Six (6/9) patients were evaluated with MRI (1.5 T Symphony, Siemmens). The study included T1 weighted FSE, GRE, STIR and T2 weighted FSE images in at least two planes (axial and coronal planes usually). We also performed time-resolved MRA sequences (DCE MRI) on 4 lesions, using 3D fast dynamic GRE imaging. We used 20 output temporal phases with a temporal resolution of 7-11 s per phase and used T1-FATSAT TSE coronal planes and a late postcontrast sequence in the axial plane. The start of the acquisition coincides with the start of intravenous contrast bolus injection. The MR imaging features are summarized in table 3.

Table 3

| Imaging Finding | | No. of tumors | Percentage |
|------------------|---------------|---------------|------------|
| Margin | Well defined | 6 | 100 |
| Contour | Smooth | 1 | 17 |
| | Polylobulated | 5 | 83 |
| Local Structures | Displaced | 4 | 66 |
| | Invaded | 2 | 33 |
| Signal Intensity | Homogeneous | 4 | 66 |
| | Heterogeneous | 2 | 33 |

The location of these tumors were intramuscular or in the subcutaneous tissue, always adjacent to a muscle fascia. They were well defined solid tumors, polilobulated and partially encapsulated.

Invasion of local structures was seen in only two cases (2/6). One tumor was located in the thigh and infiltrated adjacent bone causing internal medullar bleeding (Figure 10). In another, the tumor was located in the knee and invaded the meniscus (Figure 11).

These tumors seemed to be isointense or slightly hyperintense in T1 sequences and hyperintense in T2 and STIR sequences, compared to muscle. Signal intensity was homogeneous in four tumors (4/6) (66%) and heterogeneous in two of them (2/6) (33%). The latter were both greater than 10 cm and were diagnosed pathologically as malignant. One of them invaded adjacent bone and presented distant bone metastasis at diagnosis (Figure 12). The signal heterogeneity was caused either by necrosis or internal hemorrhage.

Four (4/9) patients were studied after intravenous contrast administration and underwent dynamic contrast enhanced sequences. The results are summarized on table 4.

Table 4

| Enhancement Finding | | No. of tumors | Percentage |
|----------------------------------|-------------------------|---------------|------------|
| Degree of enhancement | High | 4 | 100 |
| | Low | 0 | 0 |
| Enhancement pattern | Homogeneous/centripetal | 3 | 75 |
| | Heterogeneous | 1 | 25 |
| Dynamic enhancement (SI/T curve) | Biphasic curve | 3 | 75 |
| | Progressive uptake | 1 | 25 |

All tumors showed strong enhancement after gadolinium administration. Homogeneous and centripetal enhancement was visualized in three tumors (3/4) whilst only one enhanced heterogeneously (1/4) (Figure 12). This last tumor presented malignant features at pathological analysis.

In all cases a vascular pedicle was visible. In some cases the pedicle was so prominent that it could be detected in precontrast sequences as a vascular structure with signal void.

The dynamic contrast enhanced sequences showed a biphasic curve of early uptake and early washout in three tumors (3/4) (Figure 12). Two of these tumors showed benign clinical behavior and no malignant criteria, whilst the other (case 4) showed malignant behavior both clinically and at pathology.

The remaining tumor (1/4) studied presented a shallow uptake curve and a plateau washout curve (Figure 12). This tumor recurred twice during a 3 year follow up.

Four patients (4/9) were studied with CT after the administration of intravenous contrast. The lesions showed a homogeneous mass, well circumscribed, with soft tissue attenuation and heterogeneous uptake of contrast.

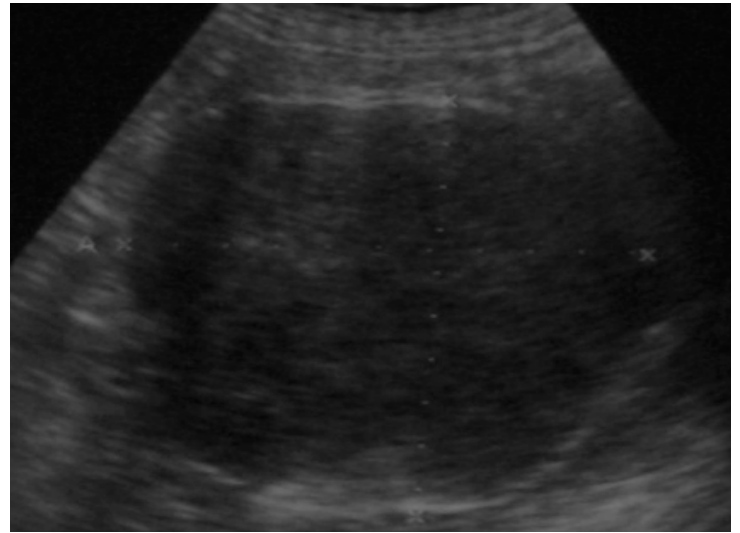
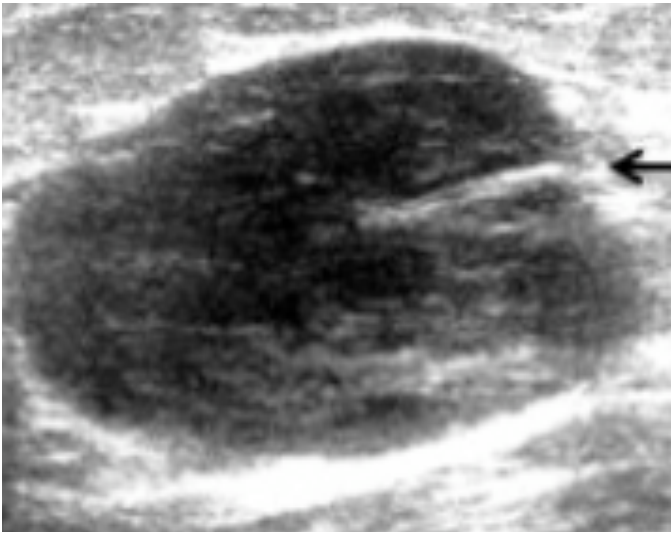


Figure 5. Well-defined masses with homogeneous hypoechoic patterns. Note the umbilical margin (arrow). Case 5 and 3.

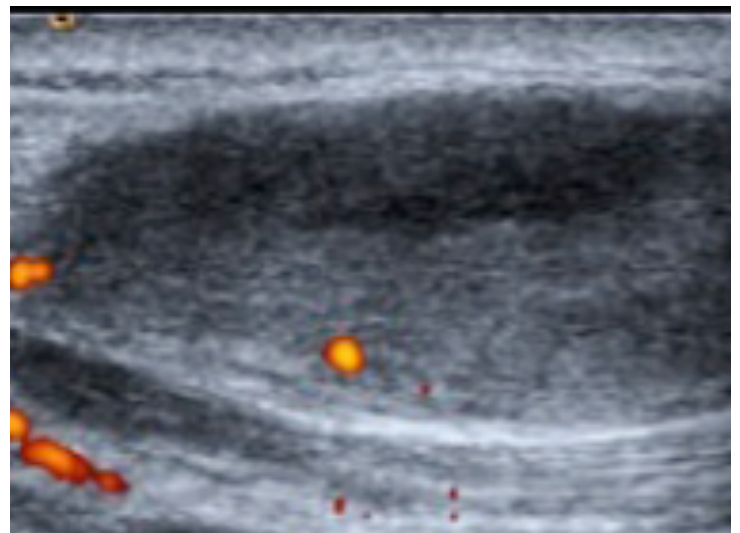
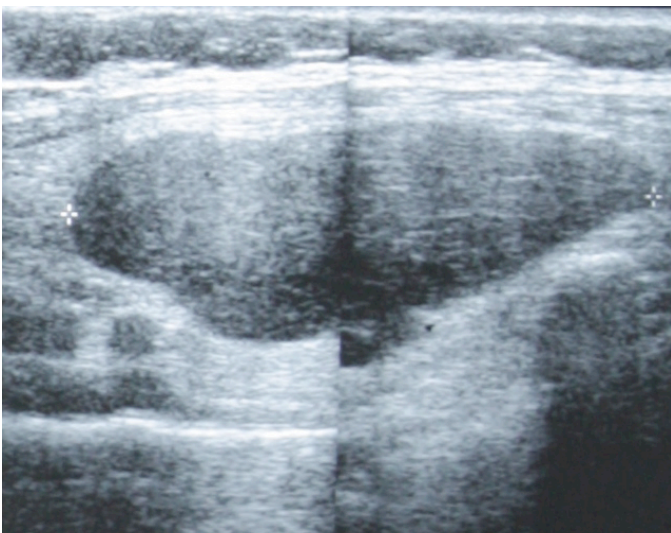


Figure 6. Well-defined mass with homogeneous hypoechoic pattern and peripheral vascularity.

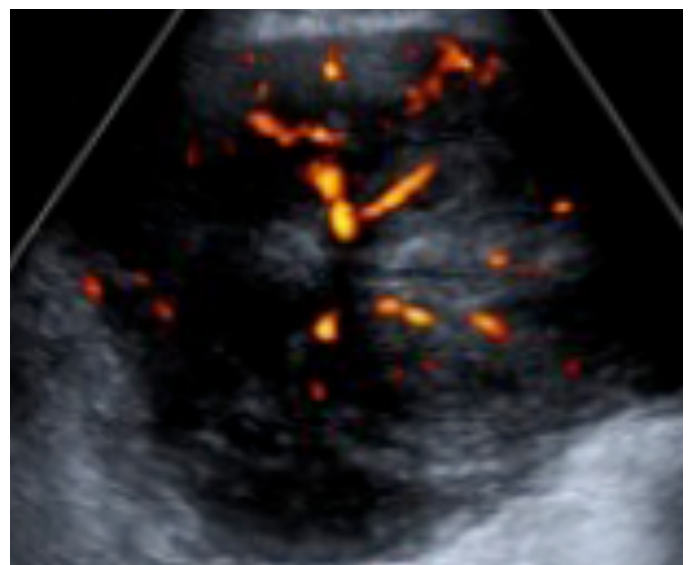
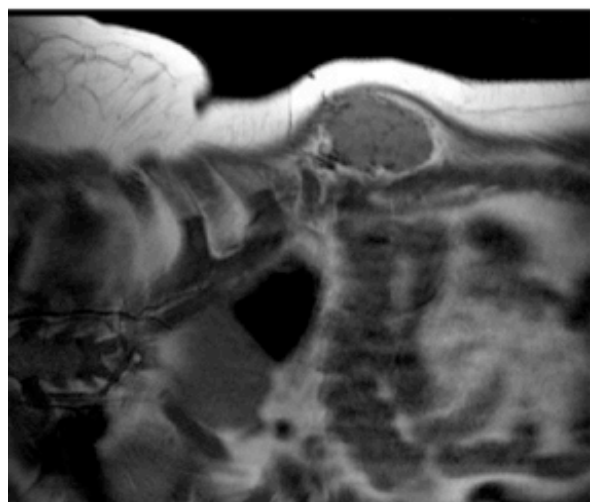


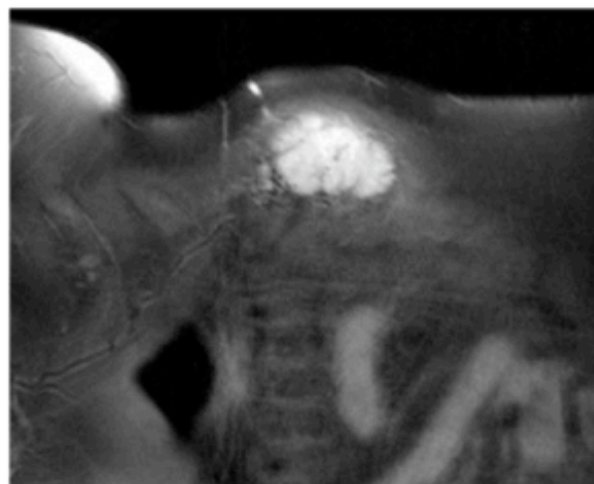
Figure 7. Well defined mass with heterogeneous ecogenicity. Power Doppler shows mass with diffuse vascularity and the presence of a vascular pedicle (arrow). Case 4.

Figure 8

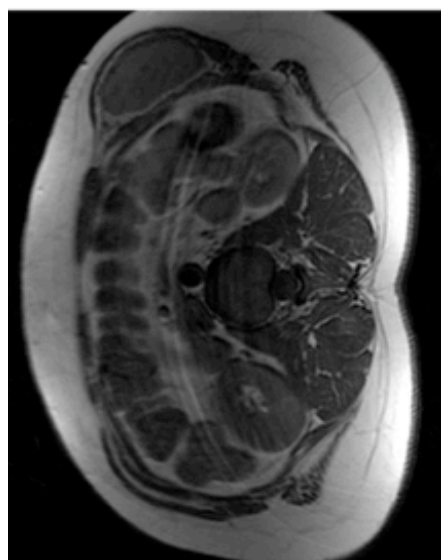
Case 1: Intramuscular abdominal wall tumor between left oblique muscles. T1 and T2 hyperintensity signal. Arterial pedicle is seen in post-contrast sequence (arrow). Homogeneous enhancement of the tumor .



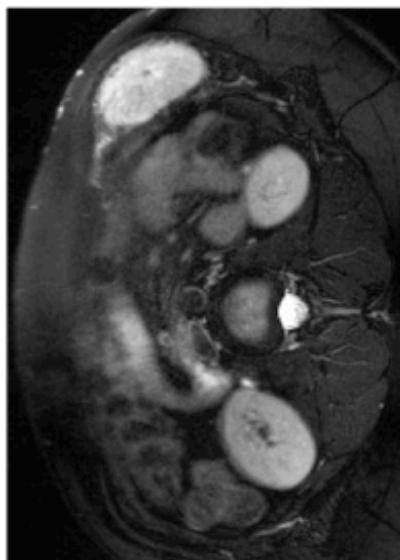
CORONAL T1



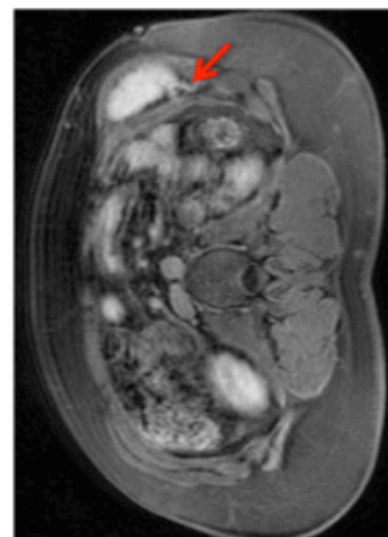
CORONAL FATSAT



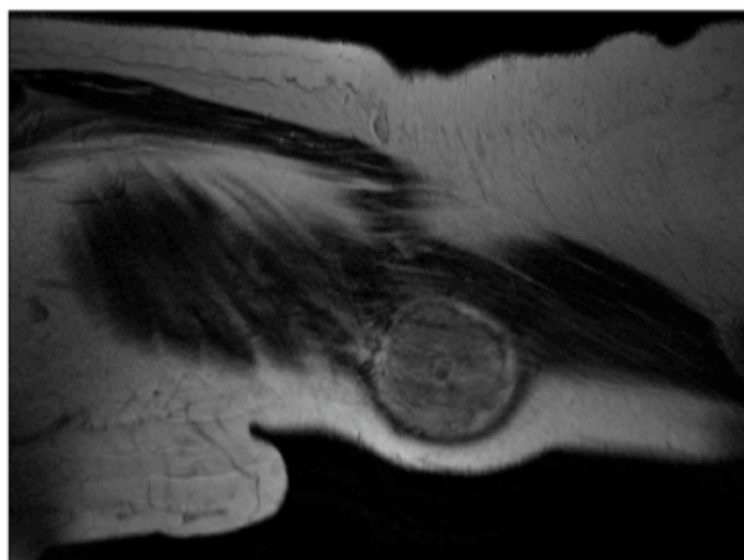
AXIAL T1



AXIAL T2



AXIAL T1 POST-GD



SAGITAL T2

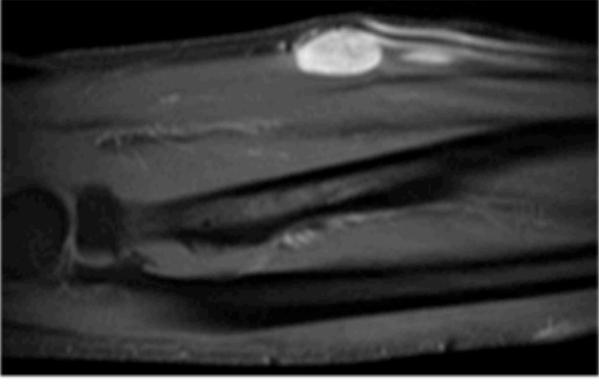
T1



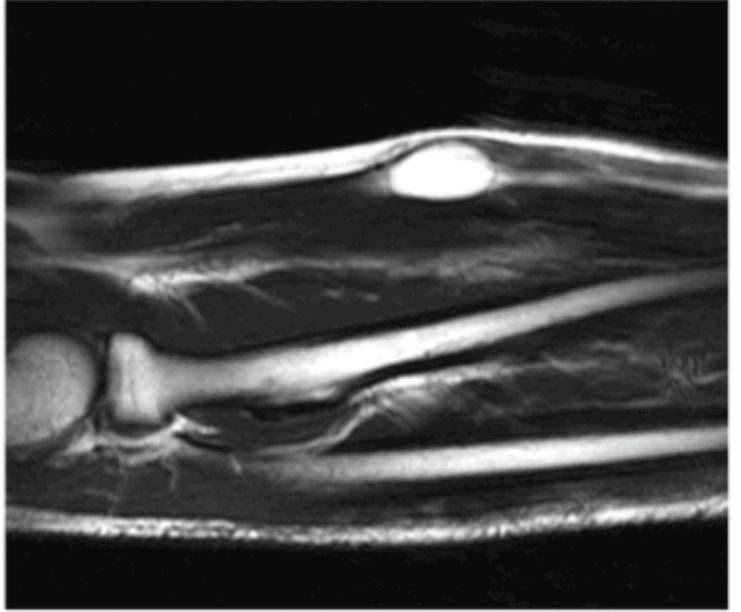
Figure 9

Case 2: Intramuscular, fusiform, well-defined and homogeneous. T1 hyperintensity signal. The curve of angiogenesis is progressive and wash out on plateau. Centripetal pattern and post-contrast with homogeneous uptake

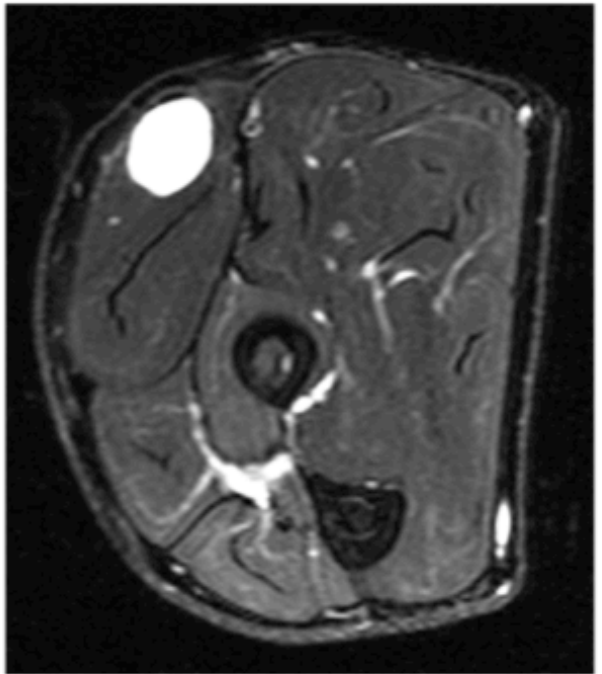
POST-GD-Late



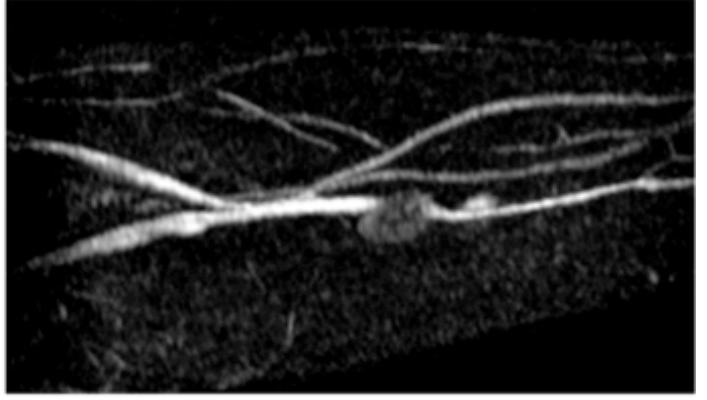
T2



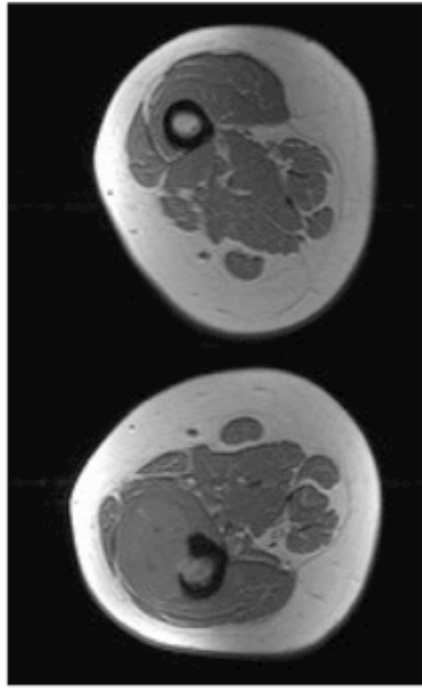
T2 FATSAT



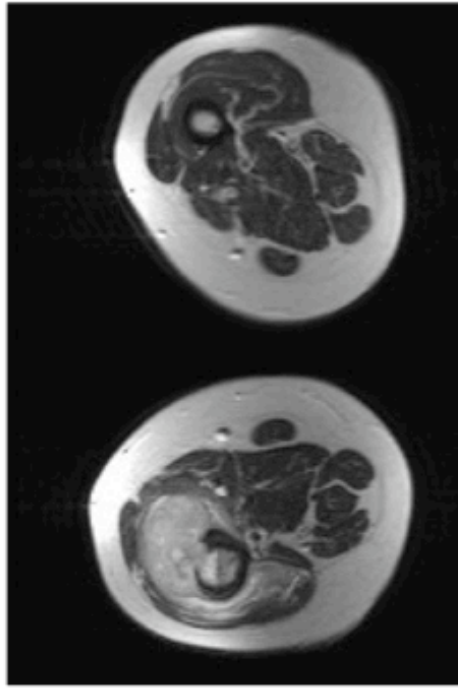
Angio-MRI-MIP



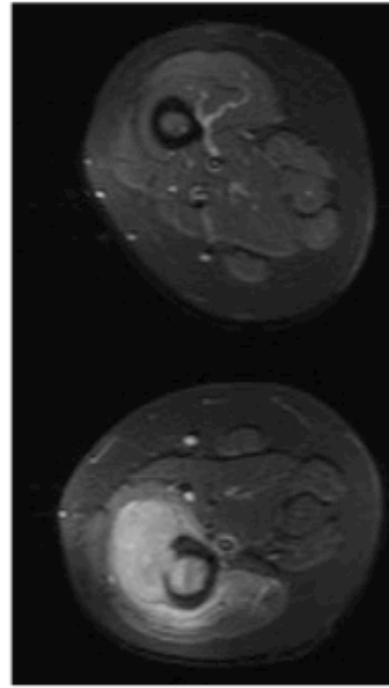
AXIAL T1



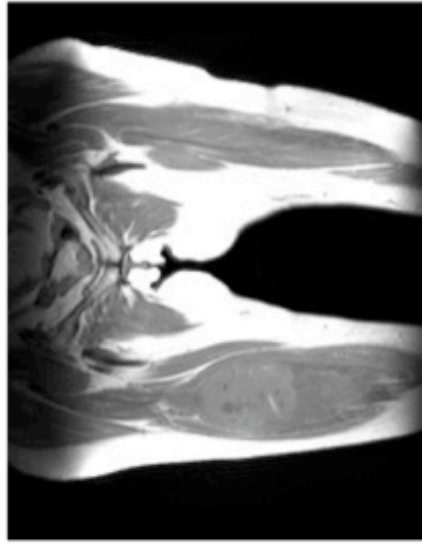
AXIAL T2



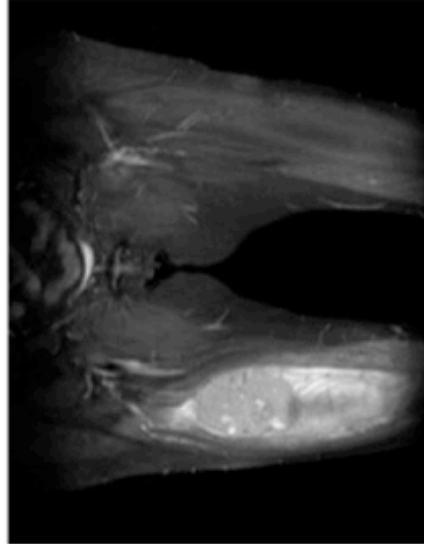
AXIAL STIR



CORONAL T1



CORONAL STIR



CORONAL STIR BONE

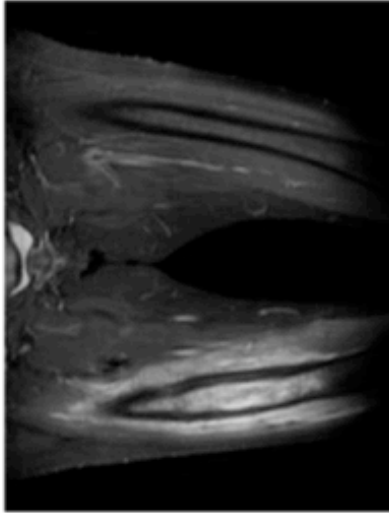
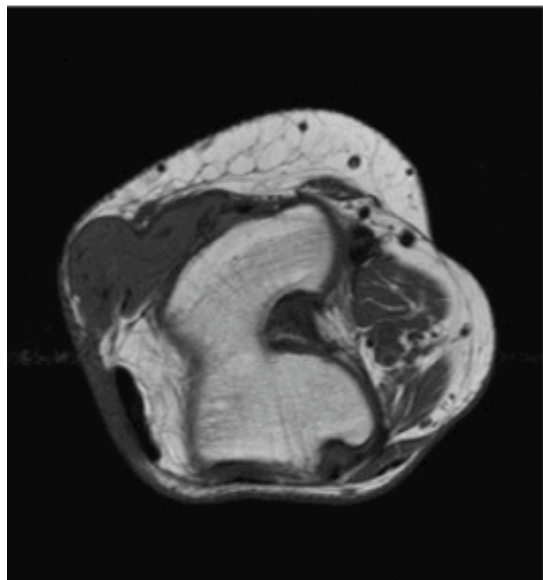
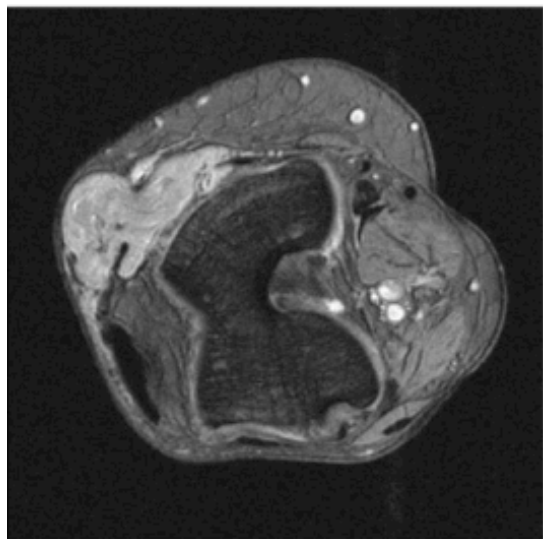


Figure 10

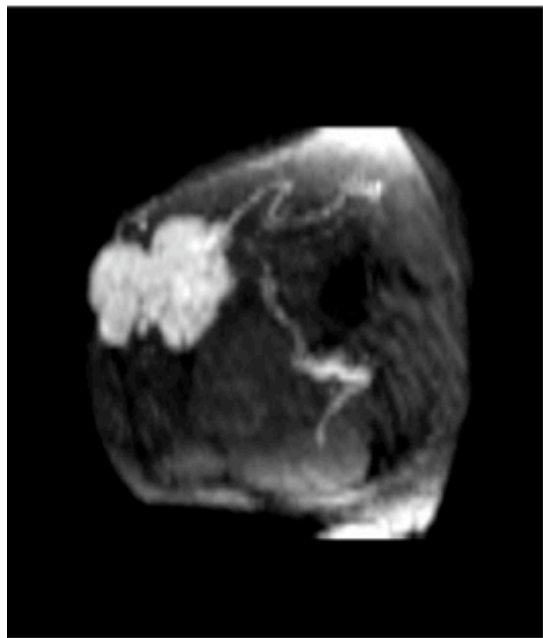
Case 4: Malignant SFT.
Intramuscular tumor in
contact with crural muscle.
Heterogeneous mass in both
T1 and T2, with internal
hemorrhage and bone
invasion.



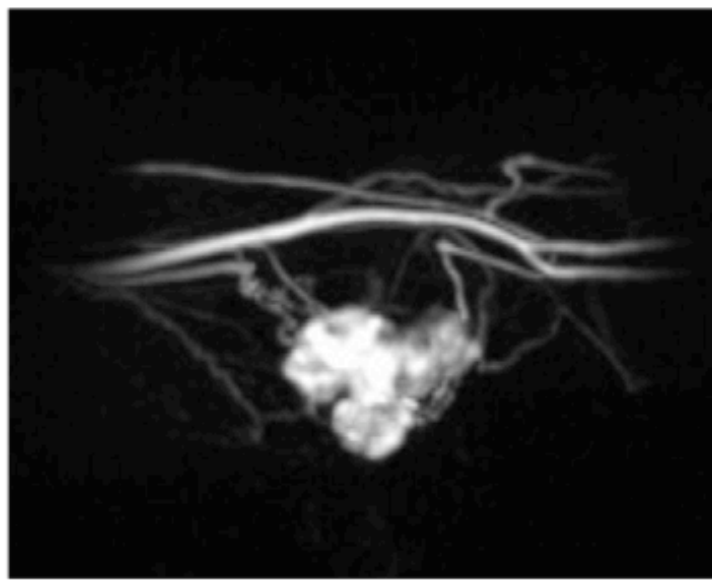
AXIAL T1



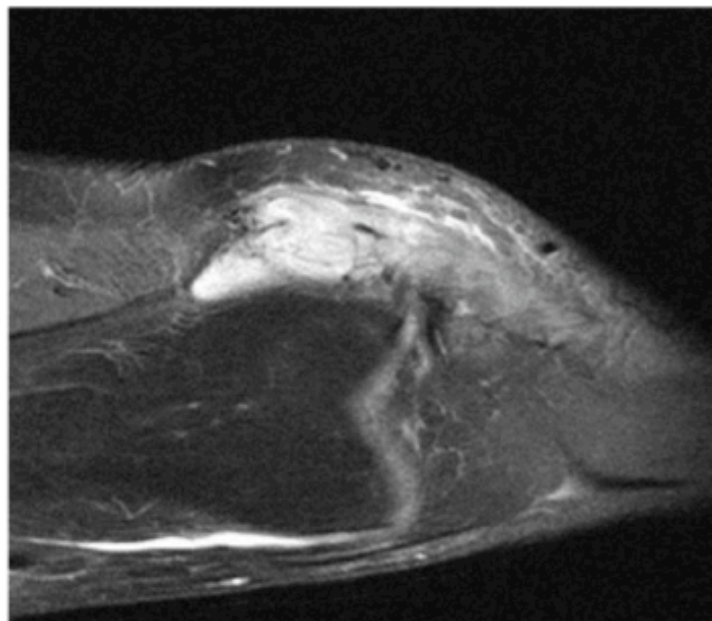
AXIAL T2



AXIAL 3D



MIP



CORONAL T2 FATSAT

Figure 11

Case 7: Well-defined tumor affecting knee cap retinaculum and intra/extracapsular fat. T1 isointense and T2 hyperintense signal intensity. Homogeneous enhancement in postcontrast late phase. Arterial pedicle and venous drainage to popliteal vessels are shown in MIP reconstruction.

Figure 12

Case 4 Malignant SFT: Radiography of the femur shows lytic lesion in diaphysis, Codman triangle and soft tissue mass. MRI image shows hyperintense lesion and metastasis in ipsilateral condyle femur. Surgical specimen shows soft tissue mass invading bone.

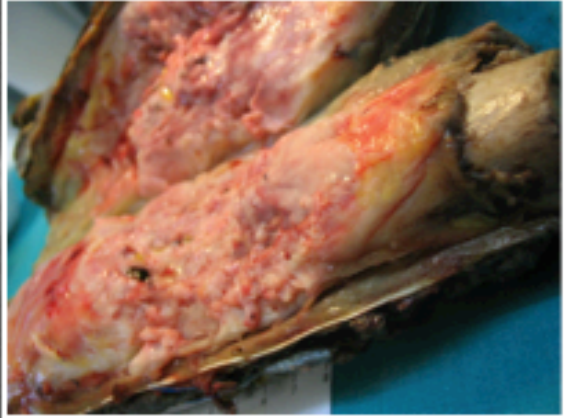
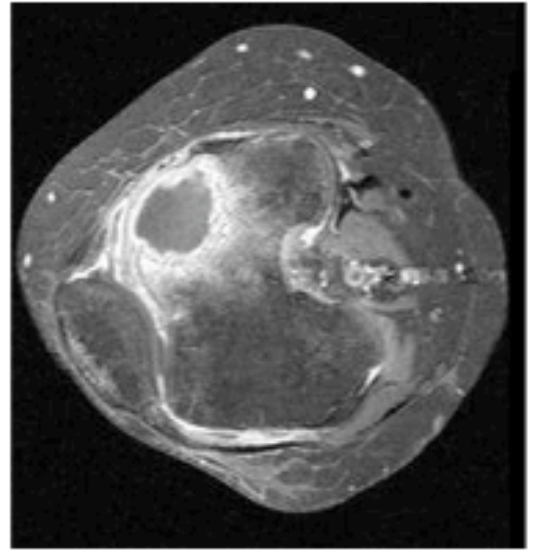
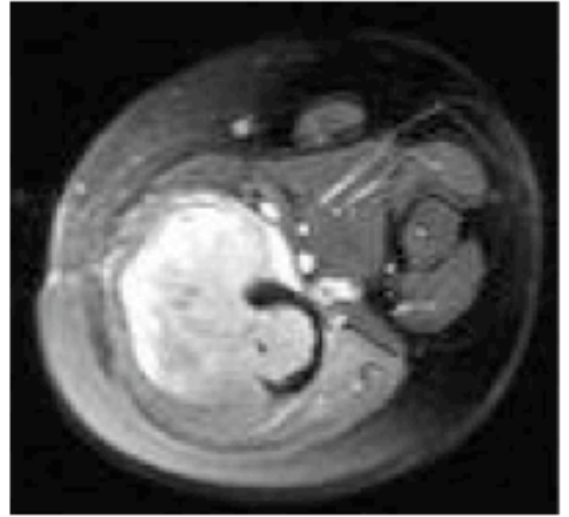
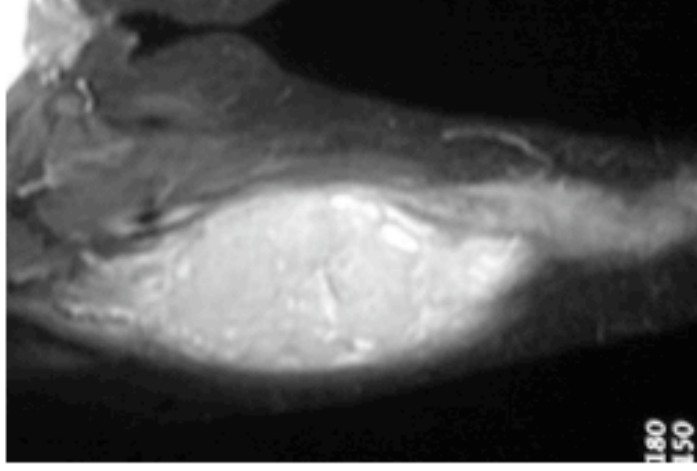
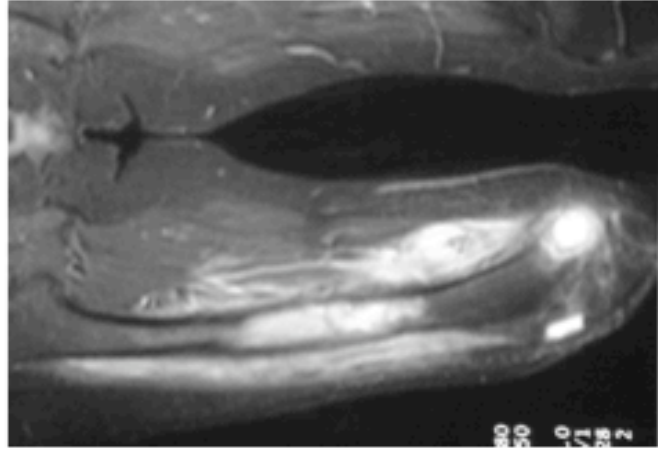
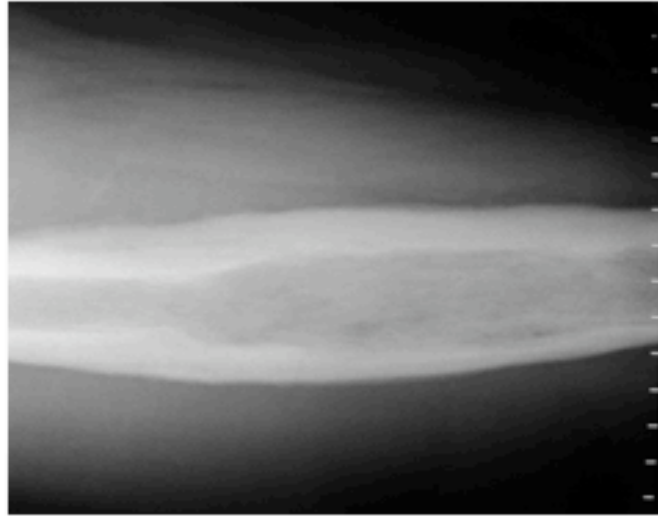


Figure 13

COMPARATIVE DYNAMIC SI/T CURVES

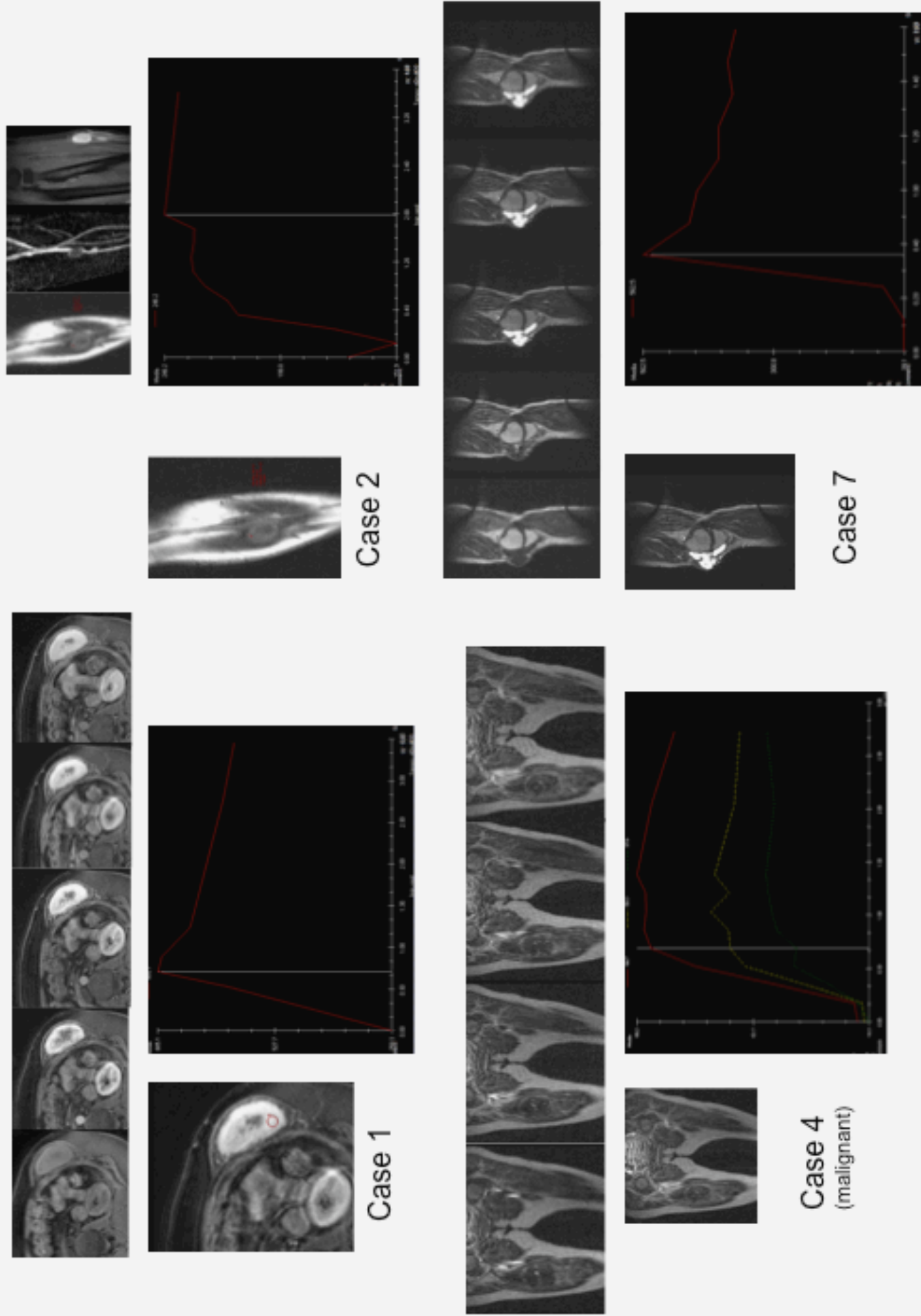
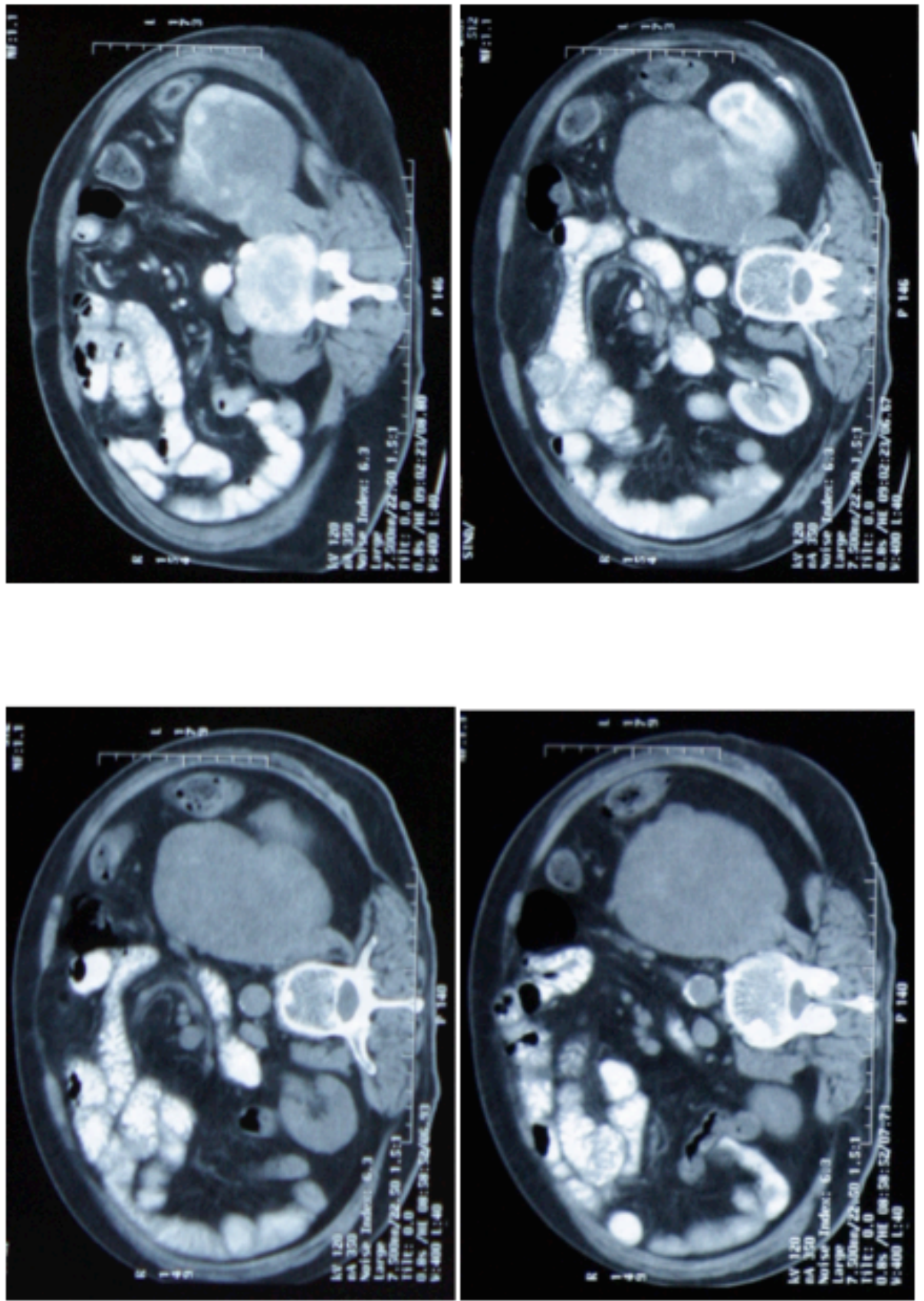


Figure 14

Case 3: CT axial images before and after the administration of intravenous contrast. Large retroperitoneal mass that displaces left kidney posteriorly and shows heterogeneous contrast uptake.



Discussion

The imaging characteristics of this tumor were not specific but in almost all cases constant. The most common findings were a well-defined, polylobulated mass that tended to displace adjacent structures. The tumors showed high vascularity in all imaging studies. Malignant tumors were indistinguishable to soft tissue sarcomas.

The radiological features that correlated better with malignant criteria were tumor size, heterogeneous signal intensity and heterogeneous uptake of contrast on MRI. These features however, did not correlate with clinical behavior (metastasis or recurrence)

Recurrence occurred in a small sized tumor (< 5 cm) that did not invade local structures and had homogeneous signal intensity. This correlates with previous literature on the unpredictable behavior of some benign looking lesions.

Metastasis was present in a large tumor (1/9) that invaded adjacent bone and showed a very heterogeneous signal on MRI sequences. This tumor presented bone metastasis at diagnosis and later developed lung metastasis.

Our study correlates with previous articles on the morphology and signal intensity of this neoplasm. The extremities are the most frequent site of presentation in our study and local structures were rarely invaded. Similar results were obtained on a recent large series study (4).

Malignant behavior in the form of metastasis and recurrence was seen in 2 tumors (2/9 22%). In a recent study, 3 patients from a series of 28 (11%) developed either metastasis or recurrence.

The differential diagnosis is broad and includes neurogenic tumors such as neurinoma or schwannoma due to their morphology, location and behavior on T1 sequences (slightly hyperintense, solid and highly vascularized). These tumors would not have a vascular pedicle.

Tumors of vascular origin would also be included such as hemangiomas, miopericytomas due to their angiogenic behavior and the presence of vascular pedicles supplying the tumor.

Finally, we would also include fibrous tumors (desmoids, fibromatous tumours) although these would be more heterogeneous and hypointense in T1 and T2 sequences, with less vascularization and different SI/T⁰ curves.

To our knowledge this is the first study where DCE MRI is evaluated in these tumors. Three tumors showed a biphasic curve and only one a progressive uptake curve. This last tumor recurred twice after extensive local surgery. Whether this distinct vascular behavior is a criteria of worst clinical outcome, is difficult to know and future studies need to be carried out with a larger series of cases.

Considering the unpredictable behaviour of this tumor, including histological benign lesions, a core biopsy and an extensive surgery should be considered. Radiological control and long-term follow up is mandatory.

The limitations of this study were the relatively short periods of patient follow up, which ranged between 2 to 5 years.

In this study a review of 9 new cases of soft tissue SFT was carried out. These tumors showed constant radiological features but unpredictable behavior. Correlation between radiological and clinical data is poor. Dynamical contrast enhanced studies might help identify those tumors with worse clinical outcome but a study with a larger series of patients is needed. Correlation between MRI features and different histological subtypes of SFTs might help improve the understanding of this rare mesenchymal tumor.

References

1. Guillou L, Fletcher JA, Fletcher CDM, Mandahl N. Extrapleural solitary fibrous tumor and haemangiopericytoma. In: Fletcher CDM, Unni KK and Mertens F, editors, World Health Organization Classification of Tumours: Pathology and Genetics of Tumours of Soft Tissue and Bone. Lyon: IARC Press, 2002:86–90.
2. Gengler C, Guillou L. Solitary fibrous tumour and haemangiopericytoma: evolution of a concept. *Histopathology* 2006;48:63–74.
3. Gold JS, Antonescu CR, Hajdu C, Ferrone CR, Hussain M, Lewis JJ, Brennan MF, Coit DG: Clinicopathologic correlates of solitary fibrous tumors. *Cancer* 2002, 94(4):1057-1068.
4. Wignall OJ, Moskovic EC, Thway K, Thomas JM. Solitary fibrous tumors of the soft tissues: review of the imaging and clinical features with Histopathologic correlation. *AJR Am J Roentgenol*. 2010 Jul;195(1)
5. Miguel Martorell, Ana Pérez-Vallés*, Francisco Gozalbo, Jose Angel Garcia-Garcia, Jair Gutierrez and John Gaona. Solitary fibrous tumor of the thigh with epithelioid features: a case Report. *Diagnostic Pathology* 2007, 2:19
6. Anders JO, Aurich M, Lang T, Wagner A: Solitary fibrous tumor in the thigh: review of the literature. *J Cancer Res Clin Oncol* 2006, 132:69-75.
7. Argyropoulou, Sivridis, Giatromanolaki, Verettas, Manavis, Argyropoulou, Malignant haemangiopericytoma of the knee joint: MR findings *The British Journal of Radiology*, 75 (2002), 539–542
8. Riss , Mamlouk, Troufléau, Depardieu et Stinès Une tumeur fibreuse solitaire de la cuisse explorée par TDM et IRM. *J Radiol* 2000; 81 : 1643-1646
9. Philip A. Dinauer, Clark J. Brixey, Joel T. Moncur, MD
Julie C. Fanburg-Smith, MD, Mark D. Murphey, MD
Pathologic and MR Imaging Features of Benign Fibrous Soft-Tissue Tumors in Adults *RadioGraphics* 2007; 27:173–187
10. Takizawa I, Saito T, Kitamura Y, Arai K, Kawaguchi M, Takahashi K, Hara N. Primary solitary fibrous tumor (SFT) in the retroperitoneum *Urol Oncol*. 2008 May-Jun;26(3):254-9. Epub 2008 Feb 20.
11. Taro Kusano & Masahiro Hayashi & Yoshiaki Hosaka Eur Solitary fibrous tumor of the inguinal region *J Plast Surg* (2007) 30:1–4
12. Moshe S. Fuksbrumer¹, David Klimstra, David M. Panicek. Solitary Fibrous

Tumor of the Liver: Imaging Findings AJR 2000;175:1683–1687

13. Catharina S. P. van Rijswijk, Maarje J. A. Geirnaerd, Pancras C. W. Hogendoorn, Antonie H. M. Taminiau, Frits van Coevorden, Aeilko H. Zwinderman, Thomas L. Pope, Johan L. Bloem, Soft-Tissue Tumors: Value of Static and Dynamic Gadopentetate Dimeglumine-enhanced MR Imaging in Prediction of Malignancy Radiology 2004; 233:493–502

14. Francesca D. Beaman, Mark J. Kransdorf, Tricia R. Andrews, MD, Mark D. Murphey, MD, Lynn K. Arcara, MD, James H. Keeling, Superficial Soft-Tissue Masses: Analysis, Diagnosis, and Differential Considerations RadioGraphics 2007; 27:509–523

15. Adrien Daigeler*1, Marcus Lehnhardt1, Stefan Langer1, Lars Steinstraesser1, Hans-Ulrich Steinau1, Thomas Mentzel2 and Cornelius Kuhnen3. Clinicopathological findings in a case series of extrathoracic solitary fibrous tumors of soft tissues. BMC Surgery 2006, 6:10

16. Krissmann M, Admas H, Jaworska M, Müller KM, Johnen G. Benign solitary fibrous tumor of the thigh: morphological, chromosomal and differential diagnostic aspects. Langenbecks's Arch Surg (2000) 385:521-525.

Akisue T, Matsumoto K, Kizaki T, Fujita I, Yamamoto T, Yoshiya S, Kurosaka M. Solitary fibrous tumor in the extremity: case report and review of the literature. Clin Orthop Relat Res. 2003 Jun;(411):236-44.

17. Taboada Rodríguez V, Zueco Zueco C, Sobrido Sanpedro C, Martínez Vicente C Solitary fibrous tumor: imaging findings and review of the literature Radiologia. 2010 Jan-Feb;52(1):67-70

18. Rosenkrantz AB, Hindman N, Melamed J. Imaging appearance of solitary fibrous tumor of the abdominopelvic cavity. J Comput Assist Tomogr. 2010 Mar-Apr;34(2):201-5.

19. Wan S, Ning L, Hong R, Wu W, Fan S, Tsuchiya H, Tomita K. Clinicopathological features of solitary fibrous tumours in the extremities: four case reports and a literature review. J Int Med Res. 2010 Mar-Apr;38(2):694-704.